Modern Chemistry
2026, Vol. 14, No. 3, pp. 85–97
https://doi.org/10.11648/j.mc.20261403.12

Research Article

Simultaneous Removal of Anionic and Cationic Dyes from Aqueous Solution Using Commercial Activated Carbon

N'guadi Blaise Allou[1, *], Corneil Quand–Même Gnamba[1], Mougo André Tigori[2], Manda Eddie–Remarck Okeu[1], Donourou Diabaté[1]

[1]Laboratory of Constitution and Reaction of Matter UFR SSMT, Félix Houphouët Boigny University, Abidjan, Côte d'Ivoire

[2]Laboratory of Environmental Sciences and Technologies of the Faculty of Environment, Jean Lorougnon Guédé University, Daloa, Côte d'Ivoire

Abstract

Synthetic dyes use in several sectors such as cosmetics, printing and textiles, can be harmful to the environment due to the lack of effluents treatment from these sectors. This study therefore aimed to contribute to the simultaneous removal of methylene blue (MB) and methyl orange (MO) from aqueous solutions using industrial activated carbon based on coconut shells. Activated carbon performance on MB and MO adsorption was evaluated by studying parameters influencing the process such as contact time, adsorbent mass, pH, temperature, initial dye concentration and adsorption selectivity. The removal rate was 99% for MB and 95% for MO after the optimal times of 10 and 20 minutes respectively. A mass of 2 g seems sufficient to remove 1 L of colored solutions of MB and MO concentrated at 50 mg L^{-1}. As far as concerning the pH, the optimal values were between 10 to 12 for MB and between 2 to 6 for MO. Furthermore, temperature had no significant effect on dye adsorption. Adsorption kinetics simulation showed that the process obeyed pseudo-second-order model following chemical adsorption while adsorption isotherm was better described by Langmuir monolayer and Freundlich multilayer models on heterogeneous surface. Langmuir model indicated maximum adsorption capacities of 21.23 mg g^{-1} for MB and 6.43 mg g^{-1} for MO. The simultaneous adsorption competitiveness of the two dyes indicated an adsorption selectivity in favor of the cationic dye. As result of this study, it appears that industrial activated carbon based on coconut shells could be safe and more effective adsorbent in MB and MO removal in aqueous media.

Keywords

Commercial Activated Carbon, Adsorption, Modeling, Cationic Dye, Anionic Dye

1. Introduction

Life on earth, including humans, animals, plants, and microorganisms, fundamentally depends on water, the most essential raw materials for sustaining life. Water availability underpins all vital processes within the biosphere. Beyond serving as both habitat and medium for energy transport, water is

*Correspondence: N'guadi Blaise Allou (alloub.neist15a@acsir.res.in)

Received: 24 June 2026; **Accepted:** 20 July 2026; **Published:** 17 August 2026

also an indispensable component of all the production systems. Nevertheless, despite remarkable technological progress, humanity has struggled to manage this invaluable resource effectively, even though it is indispensable to all forms of life. Industries, such as textiles, pigment manufacturing, leather processing, cosmetics, printing, and food processing are among the major consumers of water and organic dyes, whether soluble or pigment–based. These synthetic compounds, widely recognized for their toxicity [1, 2], may enter the food chain and pose serious risks to public health, including genetic alterations, skin redness and dryness, gastrointestinal irritation, drowsiness, cancer, and dysfunctions affecting the kidneys, liver, brain, reproductive system, and nervous system [3, 4]. Even when fixing agents are employed, substantial amounts of dyes remain in industrial effluents, making their removal prior to environmental discharge essential [5].

Regulations governing wastewater discharge have also become increasingly stringent, compelling industries to implement effective effluent treatment processes. Indeed, colored effluents are generally perceived by the public as hazardous and polluting, even though the color itself is not necessarily toxic when concentrations remain within regulatory limits. Consequently, minimizing pollution through the implementation of appropriate treatment systems incorporating a decolorization unit has become imperative. Over the past decades, numerous physical, chemical, and biological methods were developed for the treatment and decolorization of contaminated effluents. These include coagulation/flocculation [1, 6], biodegradation [7, 8], membrane filtration [9, 10], chemical oxidation [11], ozonation [12, 13], ion exchange, electrochemical methods [14, 15], and adsorption [16, 17].

Among these techniques, adsorption has emerged as one of the most widely applied and effective methods for dye removal owing to its high efficiency and operational simplicity [2]. Furthermore, adsorption–based treatment does not generate undesirable toxic effects on aquatic environments, and the adsorbent can often be regenerated and reused over several treatment cycles [18]. The principle of this process relies on trapping dye molecules onto a solid materials known as an adsorbent. Among the various adsorbents available, activated carbons remain the most effective materials for wastewater treatment because of their highly developed porous structure, large specific surface area, and remarkable adsorption capacity.

Effluents generated by textile industries generally contain at least two different dyes. Consequently, during wastewater treatment, adsorption phenomena may exhibit selective behavior toward specific pollutants. Based on this observation, the present study aimed to investigate the simultaneous removal of methylene blue (cationic dye) and methyl orange (anionic dye) using industrial activated carbon based on coconut shells as adsorbent materials. Activated carbons derived from coconut shells are much more prized due to their overall high mechanical hardness, low ash content and high micro porosity [19, 20]. These properties mainly come from the lignocellulosic character and high carbon content of the precursor material. To achieve this objective, a commercially available coconut shell-based activated carbon was employed, and adsorption experiments were conducted using both individual dye solutions and binary dye mixtures. The influence of several operating parameters, including contact time, pH, activated carbon dosage, temperature, initial dye concentration, and adsorption selectivity, was systematically evaluated. The experimental data obtained were subsequently used to investigate the adsorption isotherms and kinetics in order to better understand the adsorption behavior and mechanisms involved.

2. Materials and Methods

2.1. Materials

The activated carbon (AC) used as adsorption support in this study was a high-quality industrial granular activated carbon derived from coconut shells and supplied by Veolia (Germany). The granular activated carbon was subsequently ground using a laboratory mortar and then oven-dried for three days. Figure 1 presents the container supplied by the manufacturer, as well as the granular and powdered forms of the activated carbon. A part from activated carbon, methylene blue ($C_{16}H_{18}ClN_3S$) (Figure 1(d)), methyl orange ($C_{14}H_{14}N_3NaO_3S$) (Figure 1(e)), sodium hydroxide (NaOH) and hydrochloric acid (HCl) were used without any further purification and supplied by Chimafrique. Distilled water was used as the solvent for all experimental procedures.

Figure 1. *Container of the activated carbon supplied by the manufacturer (a), granular form of the activated carbon (b), powdered form of the activated carbon (c) and methylene blue (d) and methyl orange (e) molecular structure.*

2.2. Adsorption Parameters Study

The adsorption kinetics study was conducted to determine

the time required to reach equilibrium, a critical parameter for optimizing decolorization efficiency. For this purpose, 0.5 g of powdered activated carbon was brought into contact with 250 mL of the different methylene blue (MB) or methyl orange (MO) solutions at room temperature. The mixtures were stirred at a speed of 1500 rpm for a contact time of 180 min. For activated carbon dosage study, 50 mL of the various dye solutions at a concentration of 50 mg/L were brought into contact with different masses of activated carbon: 0.005 g, 0.01 g, 0.05 g, 0.075 g, 0.1 g, 0.15 g, and 0.25 g. The experiments were conducted at room temperature while maintaining the equilibrium contact time previously determined for each dye. The pH optimization study was carried out by introducing 50 mL of dye solutions at a concentration of 50 mg/L into Erlenmeyer flasks containing the previously determined optimal adsorbent masses. In this experiment, the effect of pH was investigated at different pH values (2, 4, 6, 7, 8, 10, and 12), measured using a HANNA Instruments HI991001 pH meter and adjusted with 0.1 M NaOH and HCl solutions. The mixtures were stirred until equilibrium was reached. To evaluate the effect of temperature on the dye adsorption process, experiments were conducted at 25°C, 35°C, 45°C, and 55°C under a stirring speed of 1500 rpm for an equilibrium time dependent on the dye used. The experiments were carried out at the natural pH of the dye solutions. For this purpose, the optimal mass of activated carbon was brought into contact with 50 mL of each dye solution at a concentration of 50 mg/L. Finally, to investigate the behavior of the activated carbon toward the different dyes at varying solution concentrations (ranging from 2 to 200 mg/L), prepared by successive dilution of the stock solutions, the dye solutions were brought into contact with the optimal adsorbent mass at their natural pH. All the withdrawn samples were filtered, and their absorbance measured using a UV–Visible spectrophotometer at the maximum wavelength (λ_{max}) of 662 nm for MB and 466 nm for MO in order to determine the residual dye concentrations. The dye percentage adsorbed and the adsorption capacity q_e (mg/g) were calculated using the following equations [17]:

$$\%\ dye\ adsorbed = \frac{C_i - C_e}{C_i} \times 100 \quad (1)$$

$$q_e = \frac{C_i - C_e}{W} \times V \quad (2)$$

In those equations, C_i (mg/L) and C_e (mg/L) represent dye initial and equilibrium concentration, respectively, V (L) and W (g) represent solution volume and adsorbent mass, respectively.

2.3. Adsorption Selectivity

The study of adsorption selectivity is a highly important parameter in adsorption processes, as it aims to determine the ability of the activated carbon (adsorbent) to preferentially retain either methylene blue (MB) or methyl orange (MO) in a binary mixture. To achieve this, two stock solutions of MB and MO were prepared at a concentration of 100 mg/L. Different MB/MO volume ratios (1/1, 1/2, 2/1, 1/4, and 4/1) were then prepared and brought into contact with the optimal mass of activated carbon. The mixtures were stirred at 1500 rpm for 20 min. Samples were subsequently withdrawn, filtered, and analyzed by spectrophotometry at wavelengths of 466 nm and 662 nm.

2.4. Structural Characterization of the Adsorbent

In order to determine the crystallinity and the nature of the functional groups present on the surface of the industrial activated carbon, two characterization techniques were employed, namely X-ray diffraction (XRD) and Fourier-transform infrared spectroscopy (FTIR). The XRD analyses were carried out using a Bruker D8 Advance diffractometer equipped with a monochromatic CuKα radiation source operating at 40 kV and 30 mA. The X-ray diffractograms were recorded over a 2θ range of 5–60° with a step size of 0.05° and a counting time of (1s/step). FTIR analyses were performed using a PerkinElmer Spectrum 2 spectrometer equipped with an attenuated total reflectance (ATR) accessory and a diamond crystal as the reflecting element. The spectra were acquired at a resolution of 4 cm^{-1} with 128 scans.

3. Results and Discussion

3.1. Characterization of Activated Carbon

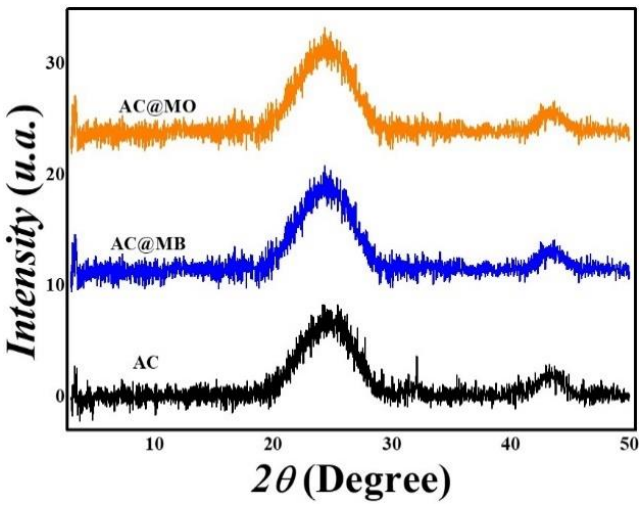

Figure 2. *X-ray diffractograms of pristine activated carbon (AC), activated carbon after MB adsorption (AC@MB), and activated carbon after MO adsorption (AC@MO).*

The results of the X-ray diffraction analysis of the activated carbon before and after adsorption of methylene blue (MB)

and methyl orange (MO) are presented on the diffractograms shown in Figure 2. The diffractogram of the activated carbon prior to adsorption exhibits a broad peak centered around 2θ = 25°, suggesting that the activated carbon possesses an amorphous or highly disordered structure, which may be associated with the crystallographic plane (0 0 2). In addition, a lower-intensity peak observed around 2θ = 43° indicates a possible transformation of the carbon toward a graphitic structure corresponding to the crystallographic plane (1 0 0) [21]. After adsorption, the diffractograms of AC@MB and AC@MO do not appear to exhibit any significant changes compared with that of the pristine activated carbon. This behavior may be attributed to the fact that MB and MO molecules did not aggregate or crystallize either on the surface or within the pores of the activated carbon [22].

Figure 3 presents the FTIR spectra of the activated carbon before and after adsorption of the different dyes. It is important to note that adsorption is often promoted by the presence of oxygen-containing functional groups on the surface of the adsorbent. The presence of functional groups on the pristine activated carbon is evidenced by the absorption bands observed between 3624 and 3930 cm^{-1}, corresponding to the vibrations of hydroxyl groups attached to the carbon surface and chemisorbed water molecules; the band at 2671 cm^{-1}, attributed to the stretching vibration of C–H bonds in aliphatic compounds; the band at 1561 cm^{-1}, associated with strong stretching vibrations resulting from a combination of aromatic C=C and carbonyl C=O bonds; and the band at 1156 cm^{-1}, assigned to C–O vibrations of ester or alcohol groups [23]. After adsorption of MB and MO, the bands around 1156 cm^{-1} and 1561 cm^{-1} not only decreased in intensity but also exhibited slight shifts. Furthermore, the appearance of a new band at 847 cm^{-1}, corresponding to the distribution of para-aromatic rings, was observed. These results clearly indicate that MB and MO dyes were successfully adsorbed onto the surface of the adsorbent.

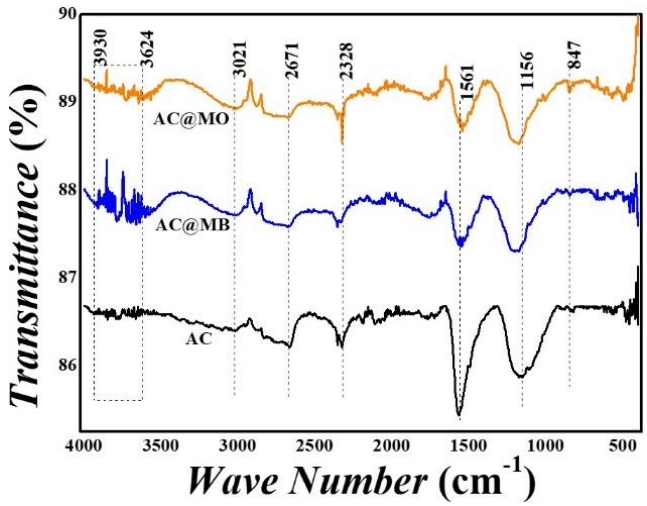

Figure 3. *FTIR spectra of pristine activated carbon (AC), activated carbon after MB adsorption (AC@MB), and activated carbon after MO adsorption (AC@MO).*

3.2. MB and MO Adsorption Optimization

3.2.1. MB and MO Adsorption Equilibrium Time

The kinetic study of methylene blue (MB) and methyl orange (MO) enabled the determination of the contact time, which is a key parameter governing dye adsorption onto industrial activated carbon [24]. The results showing the percentage of dye removal as a function of time, presented in Figure 4, reveal a three-stage adsorption process for both dyes.

An initial rapid adsorption phase was observed during the first 2 min, reaching nearly 96% dye removal for MB and approximately 47% for MO. This behavior can be attributed to the abundance of available active sites on the activated carbon surface. Subsequently, a moderate and relatively slower adsorption phase occurred between 2 and 5 min for MB and between 2 and 20 min for MO. During this stage, the removal efficiencies increased to approximately 99% for MB and 95% for MO. This phase may be explained by the progressive reduction in the number of available adsorption sites, indicating a gradual approach toward equilibrium [25].

Beyond 10 min for MB and 20 min for MO, the adsorption process reached a plateau, indicating equilibrium and, consequently, the near-complete saturation of the active adsorption sites. Therefore, throughout the remainder of this study, the equilibrium times selected for the adsorption of MB and MO onto industrial activated carbon were fixed at 10 min and 20 min, respectively.

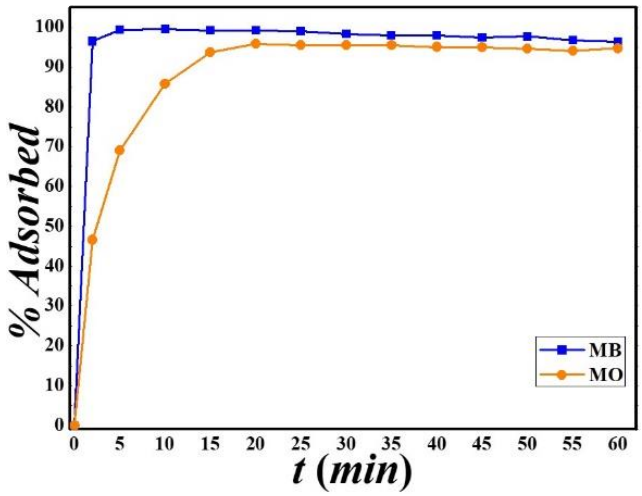

Figure 4. *Effect of contact time on the removal of MB and MO from aqueous solution using industrial activated carbon.*

3.2.2. MB and MO Adsorption Kinetic Modeling

The kinetic study of MB and MO adsorption provides valuable insight into the rate and mechanism by which the dye molecules are retained on the surface of the activated carbon. To achieve this, the adsorption kinetics were analyzed using four commonly applied kinetic models, namely the pseudo–first–order, pseudo–second–order, intraparticle diffusion, and

Elovich models [26].

The pseudo–first–order model assume that the sorption rate at time t is proportional to the difference between the amount adsorbed at equilibrium q_e and the amount q_t adsorbed at that time, and that the adsorption is reversible [27]. The linear form of its equation is given by:

$$ln(q_e - q_t) = lnq_e - k_1 t \quad (3)$$

Where k_1 (min^{-1}) is the rate constant of pseudo–first–order, q_e (mg g^{-1}) and q_t (mg g^{-1}) are the amount of adsorption at equilibrium and at contact time t.

The pseudo–second–order model, on the other hand, indicates that the adsorption mechanism of the pollutant onto the adsorbent used is chemisorption, which involves valence forces through the exchange of electrons between the adsorbent and the adsorbate [28]. The linearized form of its equation is represented by:

$$t/q_t = 1/k_2 q_e^2 + t/q_e \quad (4)$$

Where k_2 (g mg^{-1} min^{-1}) is the rate constant of pseudo–second–order.

According to the Elovich equation, solid surfaces are heterogeneous. Therefore, the adsorption rate at low surface coverage can be significantly modified by desorption or interactions between adsorbed species [27]. This model is described by equation (5), in which α (mg g^{-1} min^{-1}) is the initial adsorption rate and β (g mg^{-1}) is related to the extent of surface coverage.

$$q_t = ln\,(\alpha\beta)/\beta + ln\,t/\beta \quad (5)$$

Weber and Morris experimentally proven that, in general, there are four stages in the adsorption process by porous solids [29]: the transfer of the solute from the solution to the boundary layer around the particle, the transfer of the solution from the boundary layer to the surface of the adsorbent, the transport of the solution to the adsorbent sites: diffusion in micro pores and macro pores, and the interaction between the solute molecules and the active sites on the surface: adsorption, complexation, and precipitation. The equation is expressed as follows:

$$q_t = k_{id} t^{1/2} + C \quad (6)$$

Where k_{id} (mg g^{-1} $min^{-1/2}$) is the intraparticle diffusion rate, and C (mg g^{-1}) is a constant indicating boundary layer thickness.

The fitting results of the experimental data to these kinetic models are illustrated by the curves presented in Figure 5, while the corresponding parameters are summarized in Table 1. From these results, it can be observed that the correlation coefficient values obtained for the pseudo-second-order model were close to unity for MB and equal to 0.9996 for MO, which are significantly higher than those obtained for the other kinetic models. Furthermore, the pseudo-second-order model demonstrated that the experimentally determined equilibrium adsorption capacities were in close agreement with the calculated values ($q_{e,exp}$ = 41.81 mg g^{-1} and $q_{e,cal}$ = 42.19 mg g^{-1} for MB; $q_{e,exp}$ = 18.53 mg g^{-1} and $q_{e,cal}$ = 21.23 mg g^{-1} for MO). Taken together, these findings indicate that the pseudo-second-order kinetic model is the most suitable model for describing the adsorption of MB and MO onto industrial activated carbon. Consequently, the adsorption mechanism is likely governed by a chemical adsorption process (chemisorption), involving the formation of one or several strong chemical bonds of covalent or ionic nature between the adsorbate and the adsorbent [30].

Table 1. *Values of the kinetic parameters for the adsorption of MB and MO from aqueous solution onto activated carbon.*

Kinetic model	Parameters	Parameter values	
		MB	MO
Pseudo–first–order	$q_{e,cal}$ (mg g^{-1})	330.80	327.80
	k_1 (min^{-1})	–2.6047	–0.9374
	R^2	0.9243	0.6526
Pseudo–second–order	$q_{e,cal}$ (mg g^{-1})	42.1941	21.2314
	k_2 (g mg^{-1} min^{-1})	0.3511	0.01688
	R^2	1	0.9996
Intraparticle diffusion	k_{id} (mg g^{-1} $min^{-1/2}$)	13.254	4.1666
	C (mg g^{-1})	8.4442	2.0755

Kinetic model	Parameters	Parameter values	
		MB	MO
	R^2	0.7385	0.9377
	α (mg g^{-1} min^{-1})	1.222.10^{21}	18.7125
Elovich	β (g mg^{-1})	1.2159	0.2341
	R^2	0.8566	0.9892
Experimental data	$q_{e,exp}$ (mg g^{-1})	41.8109	18.5308

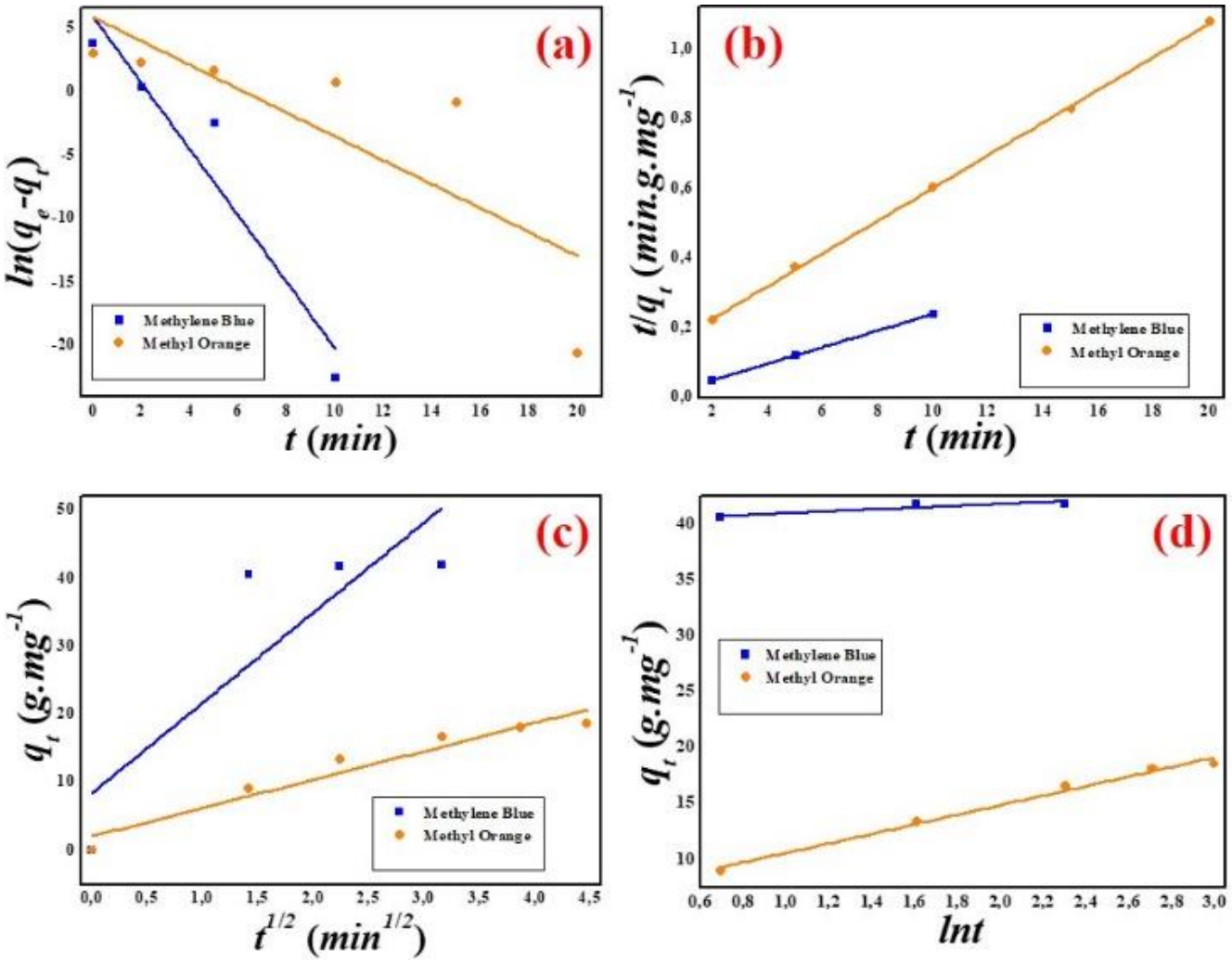

Figure 5. Kinetic adsorption plots of MB and MO using industrial activated carbon: (a) pseudo-first-order, (b) pseudo-second-order, (c) intraparticle diffusion, and (d) Elovich models.

3.2.3. Activated Carbon Dosage

It is important to note that the adsorbent dosage (activated carbon mass) strongly influences effluent removal efficiency, as it is a crucial factor governing both adsorption efficiency and the overall adsorption capacity of the process [31]. Determining the optimal adsorbent dose is therefore essential for maximizing process performance. In this context, the effect of activated carbon dosage was investigated, and the resulting trend is presented in Figure 6. The results show that the removal efficiency gradually increased with increasing activated carbon dosage [32], rising from 20% to nearly 99% for

MB and from 25% to 96% for MO. This behavior may be attributed to the increase in specific surface area, which enhances the number of available active sites for dye molecule adsorption [33, 34]. Beyond the optimal dosage, no significant improvement was observed, indicating a reduction in the availability of effective adsorption sites and a slight decrease in the adsorption percentage of MB and MO. For both dyes, an adsorbent dosage of 2 g L^{-1} can therefore be considered the optimal activated carbon dose.

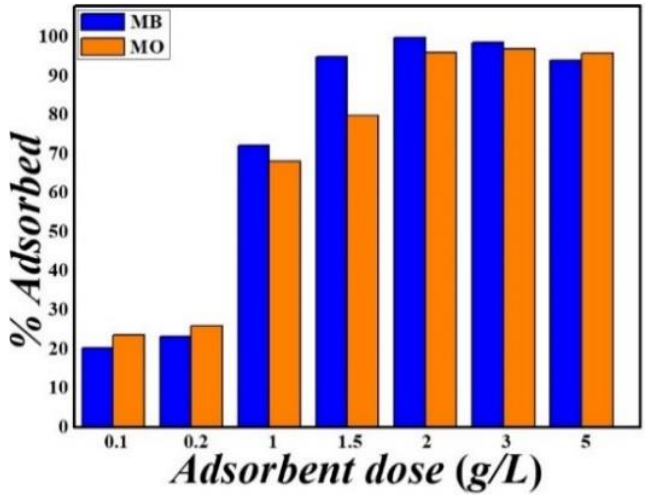

Figure 6. *Effect of industrial activated carbon dosage on the removal of MB and MO from aqueous solution.*

3.2.4. pH Influence on MB and MO Adsorption

A series of experiments was conducted to investigate the effect of pH on the adsorption process, with the aim of determining the optimal pH conditions for the adsorption of MB and MO. The results presented in Figure 7 show that the removal efficiency of MB remained close to 98–99% within the pH range of 2 to 8. At first glance, this behavior may appear to contradict conventional adsorption theory, which generally predicts electrostatic repulsion under acidic conditions. However, this observation may be explained by the particular surface characteristics of the industrial coconut shell-based activated carbon. Interactions between the adsorbent surface and MB cations, such as Van der Waals forces, hydrogen bonding, and π–π interactions [35], seem to play a dominant role and may overcome electrostatic repulsion at low pH values. At higher pH values (10–12), the removal efficiency of MB remained consistently high. Under alkaline conditions, the surface of the activated carbon becomes negatively charged due to the deprotonation of surface functional groups, thereby promoting electrostatic attraction with the positively charged MB^+ ions. This combined effect of non-electrostatic interactions and electrostatic attraction explains why the activated carbon exhibited remarkable adsorption performance over a wide pH range.

Methyl orange, on the other hand, is an anionic dye (negatively charged, MO^-). When the pH ranged from 2 to 6, the removal efficiency of MO was extremely high, approaching 100%. Under acidic conditions, the surface of the activated carbon becomes positively charged as a result of the protonation of its functional groups. This promotes strong electrostatic attraction with the negatively charged MO^- ions, thereby facilitating adsorption [36]. Consequently, the optimal pH range for methyl orange adsorption lies between pH 2 and 6. The removal efficiency of MO decreased significantly beyond pH 8, dropping to approximately 75%, before slightly increasing as the pH approached 12, reaching around 90% removal efficiency. Under alkaline conditions, the activated carbon surface becomes negatively charged, leading to electrostatic repulsion between the surface and MO^- anions, which hinders their adsorption onto the active sites [37]. Nevertheless, it should be emphasized that the activated carbon used in this study is an industrial-grade material specifically engineered to maintain high adsorption performance over a broad range of pH conditions.

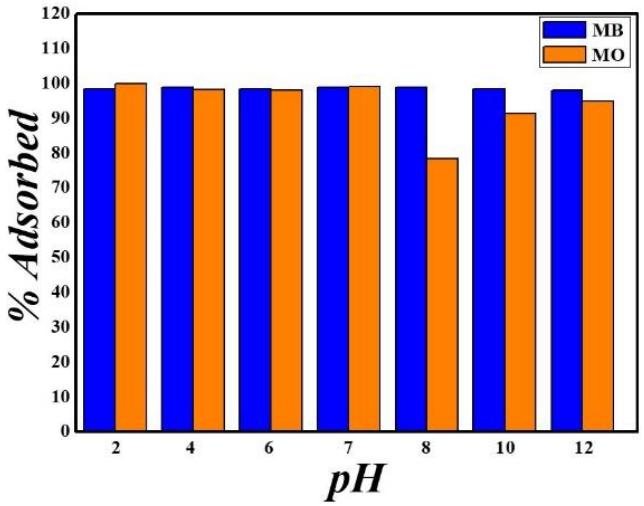

Figure 7. *Effect of pH on the removal of MB and MO from aqueous solution.*

3.2.5. Effect of Temperature on MB and MO Adsorption

The effect of temperature on adsorption may be either endothermic or exothermic and can therefore significantly influence adsorption efficiency. Increasing temperature is also known to enhance the diffusion rate of adsorbate molecules through the external boundary layer as well as within the pores of the adsorbent particles due to the reduction in solution viscosity [38]. The results obtained are presented in Figure 8.

The removal efficiency of MB remained extremely high and stable, approaching 100% over the entire temperature range investigated (25–55°C). This behavior suggests that the adsorption process is either endothermic in nature or that temperature is not the limiting factor within the studied range [39].

In contrast, MO exhibited a very high removal efficiency at 25°C, followed by a slight decrease with increasing temperature, declining from approximately 98% at 25°C to about 95% at 35°C, before progressively increasing again as the temperature approached 55°C. This behavior may indicate an exothermic adsorption process, where the thermal energy supplied to the system contributes to the partial desorption of MO molecules. Nevertheless, the overall results suggest that temperature has no significant influence on the adsorption of these two dyes when using this industrial activated carbon.

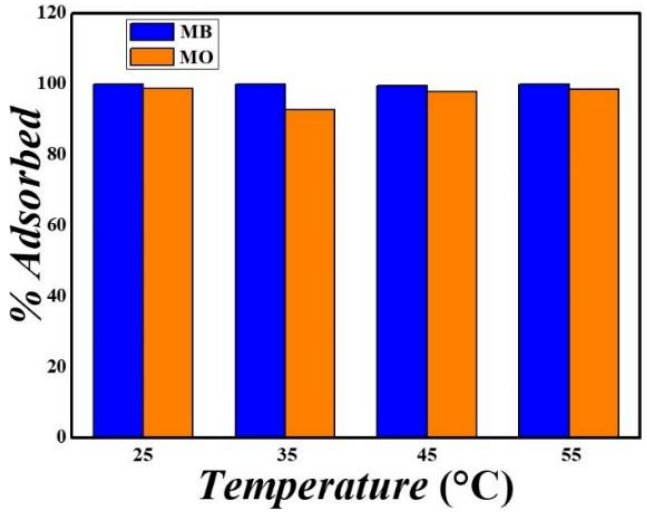

Figure 8. *Effect of temperature on the removal of MB and MO from aqueous solution.*

3.2.6. Adsorption Isotherm Modeling

The study of adsorption isotherms is essential for understanding the nature and mechanisms governing the fixation of molecules onto the surface of the adsorbent. Adsorption isotherms constitute mathematical models describing the relationship between the quantity of substance adsorbed by the adsorbent and its concentration in solution at equilibrium. To describe the adsorption process, this study focused primarily on three commonly used isotherm models, namely, Langmuir, Freundlich, and Temkin models.

The Langmuir model is based on the assumptions that a single adsorbate layer forms, that well-defined sites exist, and that there is a uniform surface with no interactions between the adsorbed molecules [27]. The linear form of the Langmuir equation is given as follows:

$$1/q_e = 1/q_m + 1/(q_m C_e k_L) \quad (7)$$

With k_L (L mg^{-1}) the Langmuir constant and q_m (mg g^{-1}) the maximum monolayer adsorption capacity.

The value of the separation factor (R_L) has chemical significance for the application of this model. It is calculated using equation (8), in which C_0 (mg L^{-1}) represents the initial concentration of the pollutant. Therefore, the process will be unfavorable if $R_L > 1$, linear if $R_L = 1$, favorable if $0 < R_L < 1$, and irreversible if $R_L = 0$ [40].

$$R_L = \frac{1}{(1+k_L C_0)} \quad (8)$$

To describe nonlinear adsorption, the Freundlich model, one of the most common isotherms in the field of adsorption, is often used. This model considers that the surface and anchoring points are diverse in terms of attachment energy, and that adsorption can occur in several layers, with possible interactions between the attached molecules [41]. The linearized form describing the Freundlich model is described by equation (9), in which k_F (mg$^{1-1/n}$ L$^{1/n}$ g^{-1}) represents the Freundlich constant indicating the adsorption capacity, and n the adsorption intensity. $1/n$ betwe en 0 and 1 suggests favorable adsorption.

$$lnq_e = lnk_F + 1/n.lnC_e \quad (9)$$

The Temkin model assumes that adsorption is a multilayer process. The Temkin isotherm explains how molecules attach to a surface. It considers the forces between molecules on the surface and in the liquid, as well as the forces between molecules already attached [42]. It also assumes that the surface energy of the adsorbent is uniform. The Temkin model is expressed as indicated by equation (10), in which $B = \frac{RT}{b_T}$ *with* b_T (kJ mol^{-1}) and A (L g^{-1}) constants of the Temkin model, R (8.314 J mol^{-1} K^{-1}) the ideal gas constant, and T (K) the absolute temperature.

$$q_e = BlnA + BlnC_e \quad (10)$$

The plots of each model are presented in Figure 9. The parameters derived from the Langmuir, Freundlich, and Temkin models are summarized in Table 2. The suitability of each model was evaluated based on the correlation coefficient (R^2) obtained from the fitting procedure. The closer the R^2 value is to unity, the better the model describes the experimental data. The Freundlich model exhibited determination coefficients of $R^2 = 0.9872$ for MB and $R^2 = 0.9486$ for MO, which are higher and closer to unity than those obtained for the other two models in the case of both dyes. These results clearly indicate that the Freundlich model provides the best description of the adsorption process for both dyes. Furthermore, the intensity factor values greater than 1 suggest that the adsorption process is favorable and occurs on a heterogeneous surface [43]. In addition, the favorable values of the separation factor ($0 < R_L < 1$) together with the acceptable correlation coefficients ($R^2 > 0.6$) for both pollutants confirm the applicability of the Langmuir model [44]. The maximum adsorption capacities were determined to be 21.23 mg g^{-1} and 6.43 mg g^{-1} for MB and MO, respectively.

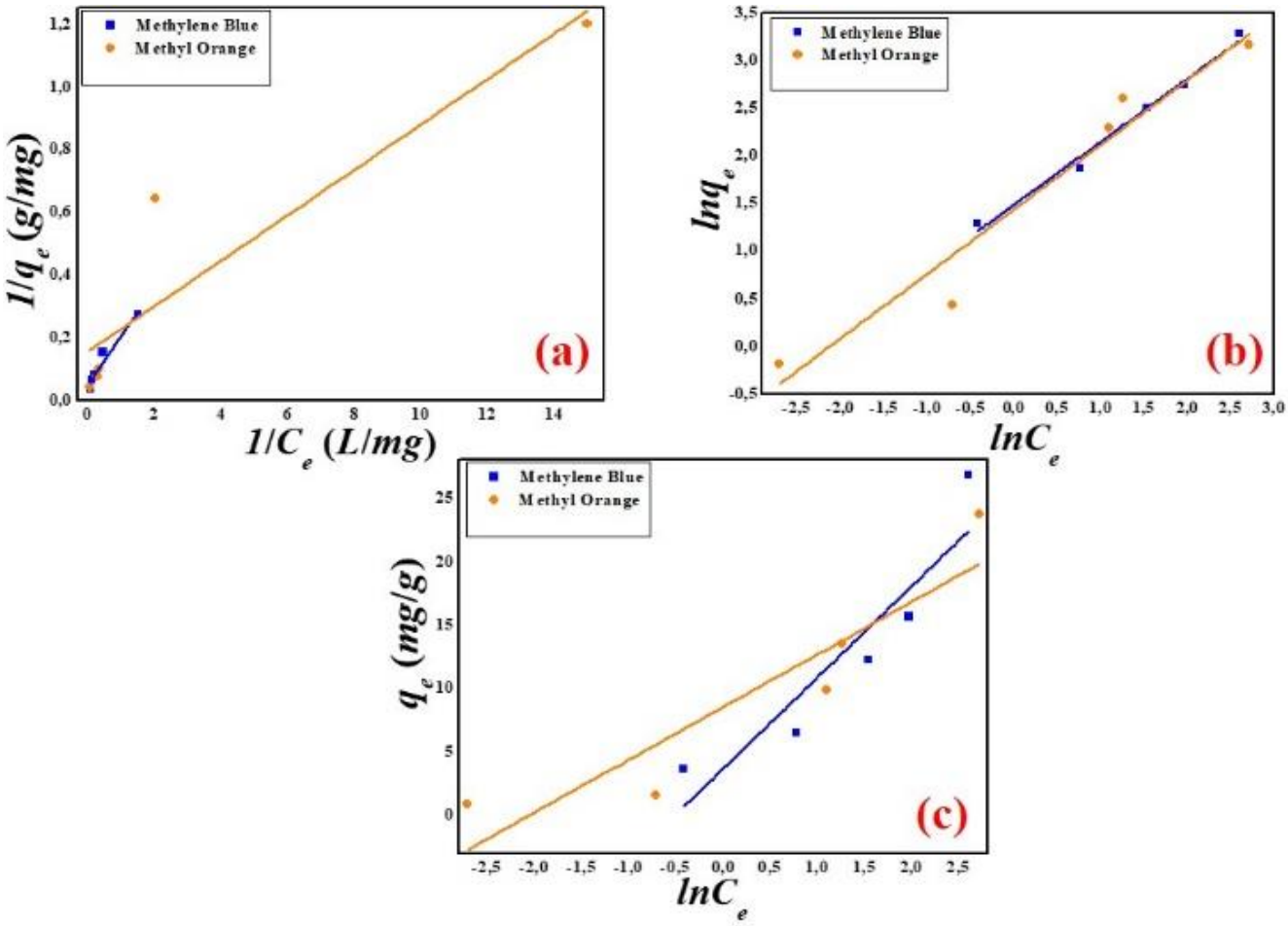

Figure 9. Adsorption isotherm plots for MB and MO from aqueous solution: (a) Langmuir, (b) Freundlich, and (c) Temkin models.

Table 2. Values of the adsorption isotherm parameters for MB and MO from aqueous solution onto activated carbon.

Isotherm models	Parameters	Values	
		MB	MO
Langmuir	$q_{max,cal}$ (mg g^{-1})	21.2314	6.4309
	k_L (L mg^{-1})	0.3025	2.1448
	R_L	0.0470–0.2932	0.0074–0.2120
	R^2	0.9511	0.9046
Freundlich	k_F ($mg^{1-1/n}$ $L^{1/n}$ g^{-1})	4.4225	4.2215
	n	1.5090	1.4767
	R^2	0.9872	0.9486
Temkin	A	11.6625	7.7887
	B	348.320	604.218
	R^2	0.8575	0.8477

3.2.7. Adsorption Selectivity Between MB and MO

To evaluate the ability of the activated carbon to remove a specific pollutant in the presence of another contaminant, an adsorption selectivity test was performed. This experiment was designed to simulate realistic wastewater treatment conditions in which several pollutants coexist simultaneously. The results presented in Figure 10 clearly reveal the existence of competitive adsorption between the two dyes. It can be observed that, regardless of the dye concentration ratio, the adsorption efficiency of MB remained consistently higher than that of MO. These findings indicate that the industrial activated carbon used in this study exhibits preferential adsorption toward cationic dyes in solution. This adsorption competition may be explained by the nature of the interactions occurring between the dyes and the activated carbon surface. MB and MO possess opposite charges, and the stronger affinity of the activated carbon toward MB suggests that π–π interactions and other non-electrostatic forces are more favorable for MB adsorption than for MO [45]. Such interactions are likely less affected by the presence of MO, thereby conferring selective adsorption toward MB. Furthermore, the surface properties of the coconut shell-derived activated carbon may provide adsorption sites that are particularly well suited for MB molecules.

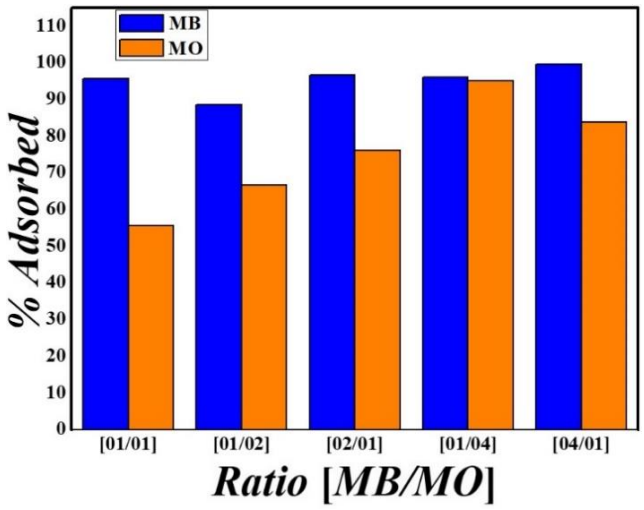

Figure 10. *Adsorption selectivity test of MB and MO in binary mixtures at different concentration ratios.*

4. Conclusion

Throughout this research project, an industrial activated carbon derived from coconut shells was used as an adsorbent for the simultaneous removal of methylene blue (MB) and methyl orange (MO) coexisting in solution, within the context of textile wastewater remediation. The results obtained from experimental investigations revealed that maximum removal of methylene blue was achieved after 10 min, whereas methyl orange reached equilibrium after 20 min on the activated carbon. Increasing the adsorbent dosage enhanced dye removal efficiency due to the increase in the number of available adsorption sites on the adsorbent surface. Therefore, the optimal adsorbent dosage was determined to be 2 g for dye solutions at a concentration of 50 mg L^{-1} for both dyes, while the pH range was found to be 2–6 for MO and 10–12 for MB. Furthermore, temperature was found not to be limiting factor affecting the adsorption efficiency of the two dyes under the studied conditions.

Kinetic and isotherm modeling results, based on the correlation coefficients obtained, indicated that the pseudo-second-order kinetic model and the Langmuir and Freundlich isotherm models provided the best fit for describing the experimental adsorption data of MB and MO onto the industrial activated carbon. The maximum adsorption capacities predicted by the Langmuir model were 21.23 mg g^{-1} for MB and 6.43 mg g^{-1} for MO. The adsorption selectivity study further demonstrated that methylene blue exhibited greater affinity toward the industrial coconut shell-based activated carbon compared with methyl orange.

In light of these findings, it is evident that the industrial coconut shell-derived activated carbon employed in this study represents a promising candidate for the simultaneous removal of MB and MO from wastewater.

Abbreviations

MB	Methylene Blue
MO	Methyl Orange
XRD	X-ray Diffraction
FTIR	Fourier-Transform Infrared Spectroscopy
ATR	Attenuated Total Reflectance
AC	Activated Carbon
AC@MB	Activated Carbon Loaded Methylene Blue
AC@MO	Activated Carbon Loaded Methyl Orange

Acknowledgments

In memory to Kouakou Vianet Bossombra, Laboratory of Thermodynamics and Physico-chemistry of the Environment, University of Nangui Abrogoua, Abidjan, Côte d'Ivoire, who did adsorbent sample characterizations.

Author Contributions

N'guadi Blaise Allou: Conceptualization, Methodology, Resources, Supervision, Validation, Visualization, Writing - orignal draft, Writing – review & editing

Corneil Quand–Même Gnamba: Data curation, Formal analysis, Investigation, Software

Mougo André Tigori: Formal analysis, Investigation, Software

Manda Eddie–Remarck Okeu: Data curation, Formal analysis, Investigation, Software, Writing – orignal draft

Donourou Diabaté: Supervision, Validation, Visualization,

Writing – review & editing

Conflicts of Interest

The authors declare no conflicts of interest.

References

[1] B. Lellis, C. Z. Fávaro–Polonio, J. A. Pamphile, J. C. Polonio, Effects of textile dyes on health and the environment and bioremediation potential of living organisms, *Biotechnology Research and Innovation* 3 (2019) 275–290. https://doi.org/10.1016/j.biori.2019.09.001

[2] P. Barciela, A. Perez–Vazquez, M. A. Prieto, Azo dyes in the food industry: Features, classification, toxicity, alternatives, and regulation, *Food and Chemical Toxicology* 178 (2023) 113935. https://doi.org/10.1016/j.fct.2023.11393

[3] J. González, M. E. Villanueva, L. L. Piehl, G. J. Copello, Development of a chitin/graphene oxide hybrid composite for the removal of pollutant dyes: Adsorption and desorption study, *Chemical Engineering Journal* 280 (2015) 41–48. https://doi.org/10.1016/j.cej.2015.05.112

[4] R. Foroutan, R. Mohammadi, B. Ramavandi, Elimination performance of methylene blue, methyl violet, and Nile blue from aqueous media using AC/$CoFe_2O_4$ as a recyclable magnetic composite, *Environmental Science and Pollution Research* 26 (2019) 19523–19539. https://doi.org/10.1007/s11356-019-05282-z

[5] R. Al–Tohamya, S. S. Ali, F. Li, K. M. Okasha, Y. A.-G. Mahmoud, T. Elsamahy, H. Jiao, Y. Fu, J. Sun, A critical review on the treatment of dye-containing wastewater: Ecotoxicological and health concerns of textile dyes and possible remediation approaches for environmental safety, *Ecotoxicology and Environmental Safety* 231 (2022) 11316. https://doi.org/10.1016/j.ecoenv.2021.113160

[6] V. Golob, A. Vinder, M. Simonič, Efficiency of the coagulation/flocculation method for the treatment of dyebath effluents, *Dyes and Pigments* 67 (2005) 93–97. https://doi.org/10.1016/j.dyepig.2004.11.003

[7] A. Rane, J. Sanket, Biodecolorization and biodegradation of dyes: A review, *The Open Biotechnology Journal* 15 (2021) 97–108. https://doi.org/10.2174/1874070702115010097

[8] B. Gurleen, A. Thakur, Distinct approaches of removal of dyes from wastewater: A review, *Materials Today Proceedings* 50 (2022) 1575–1579. https://doi.org/10.1016/j.matpr.2021.09.119

[9] C. X. Li, Y. N. Yan, F. Y. Zhou, S. P. Sun, Tailoring nanofiltration membranes for effective removing dye intermediates in complex dye–wastewater, *Journal of Membrane Science* 595 (2020) 117476. https://doi.org/10.1016/j.memsci.2019.117476

[10] M. Kabsch–Korbutowicz, M. Wolska, A. Solipiwko–Pieścik, Full–scale microfiltration for drinking water: A long–term performance analysis, *Membranes* 16 (2026) 212. https://doi.org/10.3390/membranes16060212

[11] P. Banerjee, S. Dasgupta, S. De, Removal of dye from aqueous solution using a combination of advanced oxidation process and nanofiltration, *Journal of Hazardous Materials* 140 (2007) 95–103. https://doi.org/10.1016/j.jhazmat.2006.06.075

[12] M. Khadhraoui, H. Trabelsi, M. Ksibi, S. Bouguerra, B. Elleuch, Discoloration and detoxicification of a Congo red dye solution by means of ozone treatment for a possible water reuse, *Journal of Hazardous Materials* 161 (2009) 974–981. https://doi.org/10.1016/j.jhazmat.2008.04.060

[13] D. Souza, S. M. A. Guelli, K. A. S. Bonilla, Removal of COD and color from hydrolyzed textile azo dye by combined ozonation and biological treatment, *Journal of Hazardous Materials* 179 (2010) 35–42. https://doi.org/10.1016/j.jhazmat.2010.02.053

[14] Z. M. Shen, D. Wu, J. Yang, T. Yuan, W. H. Wang, J. P. Jia, Methods to improve electrochemical treatment effect of dye wastewater, *Journal of Hazardous Materials* 131 (2006) 90–97. https://doi.org/10.1016/j.jhazmat.2005.09.010

[15] S. Raghu, C. A. Basha, Chemical or electrochemical techniques, followed by ion exchange, for recycle of textile dye wastewater, *Journal of Hazardous Materials* 149 (2007) 324–330. https://doi.org/10.1016/j.jhazmat.2007.03.087

[16] M. Hadri, Z. Chaouki, K. Draoui, M. Nawdali, A. Barhou, H. Valdés, N. Drouiche, H. Zaitan, Adsorption of a cationic dye from aqueous solution using low-cost Moroccan diatomite: adsorption equilibrium, kinetic and thermodynamic studies, *Desalination and Water Treatment* 75 (2017) 213–224. https://doi.org/10.5004/dwt.2017.20553

[17] M. Harouna, C. Tcheka, N. Dobe, Batch equilibrium and kinetic studies of anionic and cationic dyes adsorption onto Al−pillared clay from a local Cameroonian clay materials in aqueous medium, *Modern Chemistry* 8 (2020) 23–32. https://doi.org/10.11648/j.mc.20200802.12

[18] M. Vakili, G. Cagnetta, S. Deng, W. Wang, Z. Gholami, F. Gholami, W. Dastyar, A. Mojiri, L. Blaney, Regeneration of exhausted adsorbents after PFAS adsorption: A critical review, *Journal of Hazardous Materials* 471 (2024) 134429. https://doi.org/10.1016/j.jhazmat.2024.134429

[19] V. M. Cachola Maldito Lowden, M. F. Alexandre-Franco, J. M. Garrido-Zoido, E. M. Cuerda-Correa, V. Gomez-Serrano, Coconut shell-derived activated carbons: Preparation, physicochemical properties, and dye removal fromwater, *Molecules* 31 (2026) 263. https://doi.org/10.3390/molecules31020263

[20] E. H. Sujiono, D. Zabrian, V. Zharvan, N. A. Humairah, Fabrication and characterization of coconut shell activated carbon using variation chemical activation for wastewater treatment application, Results in Chemistry 4 (2022) 100291. https://doi.org/10.1016/j.rechem.2022.100291

[21] L. Yizhong, Y. Xiaoqing, C. Zhi, Y. Jingkang, X. Baorong, Y. Guidong, Design and preparation of activated carbon with high specific surface area and porosity through an organic activator coupled with CO_2 activation. In: *Advanced Materials Interfaces*, 12 (2025) 1–11. https://doi.org/10.1002/admi.202400450

[22] B. Kuppusamy, F. R. Mohamed Ismail, P. Balakrishnan, S.-C. Kim, S. P. Asrafali, T. Periyasamy, From biomass to adsorbent: A comprehensive review on bio-derived carbons for dye removal, *Polymers 18* (2026) 180. https://doi.org/10.3390/polym18020180

[23] L. Khenniche, F. Benissad-Aissani, Adsorptive removal of phenol by coffee residue activated carbon and commercial activated carbon: Equilibrium, kinetics, and thermodynamics, *Journal of Chemical & Engineering Data* 55 (2010) 4677–4686. https://doi.org/10.1021/je100302e

[24] D. Ramutshatsha-Makhwedzha, A. Mavhungu, M. L. Moropeng, R. Mbaya, Activated carbon derived from waste orange and lemon peels for the adsorption of methyl orange and methylene blue dyes from wastewater, *Heliyon* 8 (2022) e09930. https://doi.org/10.1016/j.heliyon.2022.e09930

[25] N. Semwal, D. Mahar, M. Chatti, A. Dandapat, C. Arya, Adsorptive removal of Congo Red dye from its aqueous solution by Ag–Cu–CeO_2 nanocomposites: Adsorption kinetics, isotherms, and thermodynamics, *Heliyon* 9 (2023) e22027. https://doi.org/10.1016/j.heliyon.2023.e22027

[26] S. Basu, G. Ghosh, S. Saha, Adsorption characteristics of phosphoric acid induced activation of bio-carbon: Equilibrium, kinetics, thermodynamics and batch adsorber design, *Process Safety and Environmental Protection* 117 (2018) 125–142. https://doi.org/10.1016/j.psep.2018.04.015

[27] N.B. Allou, P. Athéba, J. Saikia, K. A.-A. Soro, A. S. Ello, Methylparaben adsorption on calcined layered double hydroxides: Kinetics and isotherm modeling, *Chemical Data Collections* 57 (2025) 101187. https://doi.org/10.1016/j.cdc.2025.101187

[28] S. A. M. Idris, Adsorption, kinetic and thermodynamic studies for mercury extraction from water samples using mesoporous silica, *Modern Chemistry* 7 (2019) 58–64. https://doi.org/10.11648/j.mc.20190703.13

[29] K. M. Mousa, A. H. Taha, Study of adsorption isotherm and kinetics of reactive yellow dye on modified wheat straw, *Petroleum Science and Engineering* 1 (2017) 17–22. https://doi.org/10.11648/j.pse.20170101.14

[30] Y. S. Ho, G. Mckay, Pseudo-second order model for sorption processes, *Process Biochemistry* 34 (1999) 451–465. https://doi.org/10.1016/S0032-9592(98)00112-5

[31] C. Djilani, R. Zaghdoudi, F. Djazi, B. Bouchekima, A. Lallam, A. Modarressi, M. Rogalski, Adsorption of dyes on activated carbon prepared from apricot stones and commercial activated carbon, *Journal of the Taiwan Institute of Chemical Engineers* 53 (2015) 112–121. https://doi.org/10.1016/j.jtice.2015.02.025

[32] A. S. Ansari, F. Khan, A. Ahmad, Cauliflower leave, an agricultural waste biomass adsorbent, and its application for the removal of MB dye from aqueous solution: Equilibrium, kinetics, and thermodynamic studies, *International Journal of Analytical Chemistry* (2016) 252354. https://doi.org/10.1155/2016/8252354

[33] B. Hameed, Spent tea leaves: A new non-conventional and low-cost adsorbent for removal of basic dye from aqueous solutions, *Journal of Hazardous Materials* 161 (2009) 753–759. https://doi.org/10.1016/j.jhazmat.2008.04.019

[34] A. Jawad, N. N. M. F. Hum, A. M. Farhan, M. S. Mastuli, Biosorption of methylene blue dye by rice (Oryza sativa L.) straw: Adsorption and mechanism study, *Desalination and Water Treatment* 190 (2020) 322–330. https://doi.org/10.5004/dwt.2020.25644

[35] K. Mahmoudi, K. Hosni, N. Hamdi, E. Srasra, Kinetics and equilibrium studies on removal of methylene blue and methyl orange by adsorption onto activated carbon prepared from date pits-A comparative study, *Korean Journal of Chemical Engineering* 32 (2015) 274– 283. https://doi.org/10.1007/s11814-014-0216-y

[36] M. T. Elmorsi, Equilibrium isotherms and kinetic studies of removal of methylene blue dye by adsorption onto miswak leaves as a natural adsorbent, *Journal of Environmental Protection* 2 (2011) 817–827. http://dx.doi.org/10.4236/jep.2011.26093

[37] A. Eljiedi, A. Alseddig, A. Kamari, Removal of methyl orange and methylene blue dyes from aqueous solution using Lala clam (Orbicularia orbiculata) shell. In: *AIP Conference Proceedings*: American Institute of Physics Inc 1847 (2017) 1-7. https://doi.org/10.1063/1.4983899

[38] P. Qin, Y. Yang, X. Zhang, J. Niu, H. Yang, S. Tian, J. Zhu, M. Lu, Highly efficient, rapid, and simultaneous removal of cationic dyes from aqueous solution using monodispersed mesoporous silica nanoparticles as the adsorbent, *Nanomaterials* 8 (2018) 1-14. https://doi.org/10.3390/nano8010004

[39] Y. Kismir, Z. Aroguz, Adsorption characteristics of the hazardous dye Brilliant Green on Saklikent mud, *Chemical Engineering Journal* 172 (2011) 199–206. https://doi.org/10.1016/j.cej.2011.05.090

[40] S. Jain, R. K. Vyas, P. Pandit, A. K. Dalai, Adsorption of antiviral drug, acyclovir from aqueous solution on powdered activated charcoal: kinetics, equilibrium, and thermodynamic studies, *Desalination and Water Treatment* 52 (2014) 4953–4968. https://doi.org/10.1080/19443994.2013.810324

[41] T.–K.–C. Huynh, T.–H.–A. Nguyen, C.–H. Huynh, X.–N. Nguyen, T.–C.–T. Nguyen, H.–P. Nguyen, A.–K. Ton, T.–D. Nguyen, T. B. T. Truong, N. T. T. Tu, C. P. Trang, T.–K.–D. Hoang, Valorization of Opuntia dillenii biomass into a reusable bio-based composite for sustainable and efficient methyl orange adsorption, *RSC Advances*, 2026, 16, 26348–26371. https://doi.org/10.1039/d6ra02331b

[42] N. B. Allou, C. Q.–M. Gnamba, J. Saikia, K. E. Adou, A. S. Ello, Chemically modified tomato stems for methylene blue removal: Kinetic, isotherm and thermodynamic studies, *Next Materials* 8 (2025) 100860. https://doi.org/10.1016/j.nxmate.2025.100860

[43] F. Patiha, F. Rahmawati, S. Wahyuningsih, T. Kusumaningsih, Freundlich adsorption isotherm in the perspective of chemical kinetics (II); Rate law approach. In: *AIP Conference Proceedings*. American Institute of Physics Inc. 2237 (2020) 020037. https://doi.org/10.1063/5.0005342

[44] S. Ray, R. Gusain, N. Kumar, Adsorption equilibrium isotherms, kinetics and thermodynamics. In: *Carbon Nanomaterial-Based Adsorbents for Water Purification*: *Elsevier,* (2020) 101–118. https://doi.org/10.1016/B978-0-12-821959-1.00005-2

[45] T. H. Do, N. P. N. Nguyen, X. T. Mai, T. H. Tran, Q. D. Nguyen, T. X. Vuong, Hierarchically porous activated carbon derived from Lansium domesticum peel via hydrothermal–H_3PO_4 activation for enhanced methylene blue removal: adsorption behavior, advanced modeling and mechanistic insights, *RSC Advances* 16 (2026) 28004–28035. https://doi.org/10.1039/d6ra02695h